Published in final edited form as:
Biomaterials. 2007 August ; 28(23): 3398–3407.

Regulation of Axon Guidance and Extension by 3-Dimensional Constraints

Herbert Francisco[1], **Benjamin B. Yellen**[2], **Derek S. Halverson**[3], **Gary Friedman**[3], and **Gianluca Gallo**[1,*]

1 *Drexel University College of Medicine, Department of Neurobiology and Anatomy, 2900 Queen Lane, Philadelphia, PA 2900*

2 *Duke University, Mechanical Engineering and Materials Science, Box 90300 Hudson Hall, Durham, NC 27708*

3 *Drexel University, Department of Electrical and Computing Engineering, 3141 Chestnut Street, Philadelphia, PA 19104-2875*

Abstract

Axons *in vivo* are guided by molecular signals acting as attractants and repellents, and possibly by physical constraints encountered in the extracellular environment. We analyzed the ability of primary sensory axons to extend and undergo guidance in 3-D environments generated using photolithography. Confinement of neurons in fully enclosed square chambers decreased the percentage of neurons establishing axons as a function of chamber width. However, the ability to extend an axon in one or more directions allowed axons to form and extend similarly to those on 2-D substrata. Live imaging of growth cones interacting with the walls of chambers or corridors revealed that growth cones respond to contact with a 3-D constraint by decreasing surface area, and circumvent constraints by repeated sampling of the constraint until an unobstructed path is encountered. Analysis of the ability of axons to turn around corners in corridors revealed that the angle of the corner and corridor width determined the frequency of turning. Finally, we show that the length of axons can be controlled through the use of 3-D constraints. These data demonstrate that 3-D constraints can be used to guide axons, and control the extent of axon formation and the length of axons.

Keywords

axon; growth cone; myosin; filopodium; microfluidics

1. Introduction

During development neuronal axons are guided to their target cells by molecular signals encountered in the *in vivo* environment [1]. As axons navigate they also encounter constraints imposed by physical aspects of the cellular environment *in vivo.* Axons must ‘push’ their way through all the surrounding cells and the extracellular matrix. The size of available spaces between constituents of the extracellular matrix, termed the matrix porosity, is a determinant of axon extension. For example, axons exhibit decreased extension as a function of increased

* corresponding author Phone: 215 991 8288, Fax: 215 843 9082, Email: ggallo@drexelmed.edu

matrix porosity [2,3]. In order to overcome these physical constraints to axon extension, the tip of the extending axon, the growth cone, secretes proteases that degrade the extracellular environment allowing the axon to extend through the extracellular matrix [4]. The function of growth cone secreted proteases in allowing axons to extend through gels of extracellular matrix was demonstrated by Nordstrom et al. [5] who found that the matrix metalloproteinase stromelysin-1 released by PC12 cells was required for axon formation in gels of Matrigel, a model system for the basal lamina. Thus, although it is known that growth cones have a potential mechanism for removing at least some physical constraints imposed by the extracellular environment, the responses of growth cones and axons with physical constraints are not understood.

In vitro, axons can be guided by microfabricated grooves [6,7] and steps [8]. These observations indicate that axons respond to physical aspects of the environment, and suggest a level at which axon guidance can be controlled *in vitro* independent of molecular guidance signals. Dorsal root ganglion sensory neurons (dorsal root ganglion) provide a reliable and easy to culture primary neuronal system for the study of the regulation of axon extension. Furthermore, sensory axons in injured nerves are faced with the task of regenerating into, and being guided by, three-dimensional (3-D) tubes of Schwann cells [9], providing a rationale for investigating the interactions of sensory axons with 3-D physical constraints. In our work we investigated the ability of embryonic chicken primary sensory neurons to extend axons in a variety of environments characterized by 3-D physical constraints in the form of ‘walls’ perpendicular to the substratum the axons were growing on. We observed that 3-D constraints can regulate sensory axon formation, extension and guidance. Our observations suggest that growth cones have a mechanism for sensing the presence of a 3-D constraint and respond by redirection of their extension.

2. Methods and Materials

2.1 Generation of 3-D substrata

Three-dimensional constraints were generated using standard photolithographic techniques. We used silicon wafers (Silicon Inc. Boise, ID) with a thickness of approximately 280μm coated with a layer of the negative photoresist SU-8 10 (Microchem Inc., Newton MA). Wafers were placed on a spin coating apparatus, SU-8 10 photoresist was applied to the surface and the wafers were spun at 1500 rpm for 40 seconds to evenly coat the silicon wafer with a layer of photoresist approximately 15μm in thickness. Wafers were then pre-baked for 1.5 minutes on a hot plate at 65°C and then moved to a separate hot plate set at 95°C for 3 minutes. Following pre-baking, wafers were placed in a mask aligner, where they were brought into close contact with the electroplated metal mask. A template for the mask used in these experiments was created using the AutoCAD 2000 program, (AutoDesk Inc., San Rafel, CA). A file containing data for a mask to develop wells into SU-8 was sent to Sine Patterns LLC (Rochester, NY) where the electroplated metal mask was constructed. The mask and regions of the silicon wafer underneath were exposed to 150mJ/cm^2 of UV light, calculated from Table 3 of the Microchem information document on SU-8 photoresist formulations 2–25 found on their website at the address: http://www.microchem.com/products/pdf/SU8_2–25.pdf. Wafers were then post-baked for 1 minute at 65°C and 2.5 minutes at 95°C. Wafers were placed in SU-8 developer (Microchem Inc.) for 1 minute to remove the SU-8 that had not been exposed. The finished wafers were again placed in a deionized water bath for 2 minutes to rinse off the developing solution. Wafers were subsequently baked on a hot plate at 100°C for approximately 18 hours to remove any traces of volatile chemicals still present in the layer of SU-8. Photolithographic generation of patterns was similarly performed using german glass coverslips instead of silicon wafers for live imaging experiments.

The photolithographically patterned chips were coated with the cell growth promoting substratum laminin prior to plating cells. Each chip therefore contained varied arrays of chambers and corridors containing 3-D constraints in the forms of "walls", and a large "top" 2-D surface without 3-D constraints. We created square chambers and corridors of different sizes. The soma of dorsal root ganglion neurons under our culturing conditions is approximately 20 μm in diameter. Thus, we investigated the effects of complete spatial 3-D confinement in square chambers ranging from 40×40–120×120 μm on the ability of neurons to establish axons. Similarly, to determine the effects of constraints in two out of four possible directions of axon advance, we studied the response of neurons to confinement in long (700 μm) corridors with widths ranging between 20–50 μm. The height of the walls of chambers and corridors was kept uniform at 15 μm. For all experiments, the neurons were cultured for 24 hrs prior to fixation, immunocytochemical staining and data acquisition.

2.2 Culturing and reagents

All neurons used in these experiments were obtained from the Dorsal Root Ganglia (DRGs) of embryonic day 10 chicken embryos. DRGs were dissected according to standard protocol [11] and placed in 5mL of Ca^{2+}/Mg^{2+} free (CMF) Phosphate Buffered Saline (PBS) (Invitrogen, Carlsbad, CA) for 10 minutes at 37°C to disrupt Ca^{2+} dependant cell adhesion mechanisms. After 10 minutes DRGs were spun at 3100 rpm for a few seconds to obtain a pellet. The CMF-PBS was aspirated off and 5mL of 0.25% Trypsin-EDTA (Gibco Cell Culture Systems) was added. DRGs were incubated in trypsin for 10 minutes at 37°C after which they were spun for one minute to collect the pellet, the trypsin was aspirated off, and 5mL of Ham's F12 Medium (Mediatech Inc. Herndon, VA) with 10% Fetal Bovine Serum (BioWhittaker, Inc. Walkersville, MD) and 10 mM HEPES (from Sigma) (F12HS10) was added. DRGs were then dissociated by pipette mediated fluid shear trituration. The dissociated cells were next pelleted after which the F12HS10 was aspirated off and Ham's F12 Medium with additives [see 9] containing 20 ng/mL of nerve growth factor (R&D Systems, Minneapolis, MN) was used to resuspend the dissociated cells prior to plating. Blebbistatin was purchased from Toronto Research Chemicals (North York, Ontario Canada) and dissolved in DMSO (25 mM stock). Culturing surfaces were coated overnight at 39°C using 25 μg/mL laminin (Invitrogen, Carlsbad CA) in PBS.

2.3 Immunocytochemistry

In order to determine neuronal morphology cultures were stained with anti-tubulin antibodies to clearly reveal axons. After 24 hours of incubation, cell cultures were fixed with 0.25% gluteraldehyde for 15 minutes. The fix solution was then removed and 2mg/mL sodium borohydride in CMF-PBS was applied for 15 minutes to quench residual fixative. The cultures were then blocked with 10% Goat Serum + 0.1% TX-100 in PBS and stained with fluorescein conjugated anti-α-tubulin (Sigma) at 1:100 dilution in 10% goat serum in PBS, for 1 hour. Cultures were also counter stained with rhodamine phalloidin to reveal actin filaments, following the manufacturer's protocol (Sigma). To minimize photobleaching, coverslips were mounted in nofade and stored at −20°C [9].

In order to determine the amount of laminin bound to SU-8 and silicon oxide substrata, the substrata were coated overnight with 25 μg/mL laminin in the same dish in order to minimize experimental variation. Control substrata were not coated with laminin but placed overnight in PBS, the vehicle for laminin. Substrata were fixed with 0.25% gluteraldehyde for 15 minutes and processed as described for tubulin staining. Substrata were stained with anti-laminin antibodies (1:50, Sigma) and then with rhodamine conjugated secondary antibodies. Images of the stained substrata were collected from all groups (20 fields, 20x magnification). The mean intensity of staining within group (SU-8 or silicon oxide) was determined. In order to correct for differences in background due to intrinsic substratum autofluorescence and non-specific

antibody staining, the mean of the no-laminin, but antibody stained, control substrata was subtracted from that of laminin coated substrata. The background-subtracted values were then compared using a Welch t-test across SU-8 and silicon oxide.

2.4 Live imaging

DRG neurons were dissected and dissociated as previously mentioned and cultured for 5 hours on the surface of the photolithographically patterned coverslips. Neurons on patterned coverslips were cultured in Falcon 1008 dishes. Coverslips were imaged with a Zeiss Axiovert 135M using a 20x phase objective and 2 hour videos were taken using Axiovision imaging software and a Zeiss Axiocam at 1 minute intervals. An Air Stream Stage Incubator (Nevtek) was used to maintain cultures at 39°C during imaging. Changes in growth cone area were determined using the area-of-interest function in Zeiss Axiovision software. Briefly, the phase bright lamellipodia were included in the measurement of lamellipodial area, excluding the phase dark central domain of the growth cone [13].

2.5 Analysis of axon formation and length in chambers and corridors

Cells were cultured for 24 hours on photolithographically patterned wafers before being fixed, stained with tubulin antibodies and viewed using epi-fluorescence microscopy (Zeiss 200M microscope, 20x objective). The effect of spatial constraints was analyzed in these cultures by determining the ratio of the percentage of neurons with axons within square wells and rectangular corridors relative to the percentage of neurons with axons on the upper surface of the SU-8 layer of the same culture, termed the periphery (Figure 1A, B). Thus, if neurons in chambers grew axons as frequently as the control neurons in the periphery then a value of 1 would be obtained, indicating no effect of confinement. Throughout the paper, the term percentage of neurons with axons in the context of chambers and corridors thus reflects on the ability of neurons in confinement to grow axons relative to neurons growing on a 2-D substratum without physical constraints. Square wells with sides ranging from 40μm to 120μm, and long rectangular chambers of 30μm to 50μm in width and over 700μm in length, were analyzed in a similar manner, with changes in the ratio of cells exhibiting axons in 10 chamber arrays being noted as a function of chamber width. Within chambers, we did not observe a relationship between placement of the cell body and whether the neuron had extended an axon (for example compare Figure 1D and E).

The length of axons was determined by digitally tracing the entire length of the axon using the measurement module of Zeiss Axiovision Software, thereby providing a direct metric of total axon length.

2.6 Analysis of axon turning around corners

Cells were cultured on silicon wafers with patterned layers of SU-8, fixed after 24 hours and stained with anti-tubulin antibodies. Axons projecting from cell bodies within 100μm of an angle were observed and quantified in terms of whether or not they projected around the corner (see Figure 5A for examples). The distance of 100μm was chosen because in corridors axons on average project approximately 500μm in 24 hours. Cells within 100μm extending axons toward a corner are thus predicted to, on average, have ample time to interact with the corner prior to fixation and analysis.

3. Results

3.1 3-D spatial confinement of neurons

In order to study the behavior of primary dorsal root ganglion axons and growth cones in environments containing 3-D constraints, we used photolithography to generate 3-D

environments on silicon chips (Figure 1A). We first determined the percentage of neurons that grew axons when confined in square chambers of varying sizes, and expressed it as a ratio to the percentage of neurons growing axons on the 2-D substratum of the chips in the vicinity (100 μm) of the arrays of chambers (periphery, Figure 1A, B). If neurons in chambers grew axons as frequently as the control neurons in the periphery then a value of 1 would be obtained, indicating no effect of confinement. The percentage of neurons in square chambers that grew axons was dependent on the size of the square chamber (ANOVA, $p<0.05$; Figure 1C and D). Direct comparison between the percentage of neurons growing axons in chambers between 40×40 to 70×70 μm, and neurons on the 2-D substratum adjacent to the chambers, revealed statistically significant differences at all chamber sizes ($p<0.05$ for each comparison, Welch t-test). Figure 1E shows an example of a neuron in a chamber that did not grow an axon.

We observed that approximately 10% of all neurons in chambers exhibited ‘escapee’ axons that had grown up the walls of the chambers and extended onto the available nearby 2D substratum (Figure 1F). These ‘escapee’ axons were not considered in our analysis, but provided evidence that confinement per se was not inhibitory to axon formation or maintenance, consistent with the study of Li and Folch [8]. Rather, if territory lacking 3-D constraints was available, due to the axon having grown over the wall of the chamber onto the top layer of the chip, then the axon could extend even if the cell body was confined.

Confinement within long corridors did not affect the percentage of neurons growing axons relative to neurons grown on a 2-D substratum. In corridors, axon formation from the cell body was constrained in only two directions by the walls of the corridor, with the remaining two directions not providing 3-D constraints on axon extension. Although a slight trend toward more neurons having grown axons in corridors between 20–50 μm was observed, no statistical differences were obtained comparing the data (Figure 1C; ANOVA, $p>0.05$). Collectively data from rectangular and square chambers indicate that confinement has no significant effect on the initial growth of axons when at least two directions are available for extension without spatial constraints (rectangular chambers), but significant impairment in the growth of axons is observed under conditions of confinement in all directions (square chambers).

In our culturing system, axons growing in the chambers and corridors are extending on a laminin-coated silicon oxide substratum, while those growing on the top of the chip are extending on a laminin-coated SU-8 substratum. The observation that as a function of chamber size the percentage of neurons growing axons within chambers with a silicon oxide substratum attains a similar level as those growing on the SU-8 layer (Figure 1C, chambers greater than 80×80 μm) indicates that the two substrata, laminin coated SU-8 and silicon oxide, are equally permissive for axon growth as long as a minimal area of substratum is available without physical constraints. Regardless, we determined the amount of laminin bound to the silicon oxide and the SU-8 layers by quantifying the intensity of immunochemical staining of laminin-coated substrata (details in Methods and Materials section 2.3). Laminin immunostaining levels were 60% higher on SU-8 than silicon oxide ($p<0.01$ Welch t-test, n=20 fields per substratum). In order to verify that the amount of laminin on both substrata is sufficient to promote axon formation from neurons with similar potency we compared the percentage of neurons extending axons on two-dimensional SU-8 or silicon oxide substrata coated with laminin. This analysis revealed that although less laminin bound to silicon, neurons were similarly able to grow axons on both substrata. On SU-8 and silicon oxide, 61% and 58% neurons grew axons, respectively (n.s., X^2 test, $n>1400$ neurons per group). Thus, the difference in the ability of neurons to extend axons in chambers and corridors relative to the top surface of the chip is not attributable to differences between the two substrata. These control experiments support the conclusion that the major determinant of axon extension in our experiments is the presence of 3-D constraints to axon extension (Figure 1).

3.2 Inhibition of myosin II

Myosin II is an important cellular mediator of the responses of growth cones and axons to molecular signals that inhibit axon growth and establishment [11]. In order to gain insights into the cellular mechanism by which 3-D constraints decrease the establishment of axons, we cultured neurons in the presence of the myosin II inhibitor blebbistatin (75 μM) [12] and determined the extent of axon formation in small chambers. Inhibition of myosin II allowed neurons to establish axons in 40–50 μm wide chambers (Figure 2; $p<0.05$ for comparisons between blebbistatin and DMSO control treated cultures). Myosin II inhibition by itself did not alter the establishment of axons by neurons on 2-D substrata ($p>0.55$, Welch-test, $n>10$ cultures per group, blebbistatin and DMSO treatment). These data indicate that myosin II activity is required for the inhibitory effects of spatial constraints on axon formation.

3.3 Determination of axon length

In order to determine if spatial constraints can control the extent of axon extension, we compared the lengths of axons in 40 μm wide rectangular chambers to those in rectangular 40×40 μm chambers in series connected by “doors” (discrete areas in rectangular chambers where chamber width narrowed; Figure 3A and B). Doors are described by their width and length (Figure 3A). We hypothesized that the inclusion of doors in corridors would slow down axon extension by imposing a physical constraint on axon extension demanding that the growth cone navigate around the constraints until a path for continued advance is discovered (Figure 3B). To determine whether axon length could be manipulated by inclusion of “doors” in chambers, we measured the length of axons in 40μm rectangular chambers with doors of varying length (5–25μm) and width (8 and 15μm) and compared these data to control axons extending in 40μm width rectangular chambers with no doors. Altering door width between 8–15 μm had no statistically significant effect on average axon length (data not shown). Significant differences in axon outgrowth were obtained comparing control rectangular chambers with no doors and rectangular chambers with door lengths of 5μm, 10μm and 15μm (Figure 3C). In these groups neurons had axon lengths that were approximately 30% shorter than the control axons. Doors of greater length resulted in axon lengths not different from controls.

Approximately 40% of axons growing in long rectangular chambers without doors grew to the end of the chamber, thus the measurement for average axon length in 40μm chambers is likely an underestimate of the average axon length in these chambers. By contrast, the majority (~90%) of axons extending in long chambers with doors did not contact the end of the chamber. Collectively, the data demonstrate that the length of axons can be controlled by the design of appropriate 3-D constraints. Thus, 3-D constraints can be used to control both the percentage of neurons establishing axons, and to regulate the length of axons that form.

3.4 Live-imaging of growth cones

In order to directly determine the behavior of growth cones encountering 3-D constraints we generated chambers interconnected by doors on glass coverslips (Figure 4A). This allowed us to use phase contrast microscopy to track the behavior of living growth cones before and after contact with 3-D constraints, the walls of the chambers. Dissociated DRG neurons were plated on photolithographically patterned glass coverslips and incubated for 5 hours, after which the live cells were imaged. Axon extension within rectangular chambers containing a series of 8–15μm doors ranging from 5–25μm in length was recorded and the behavior of growth cones encountering spatial constraints, the walls of the corridor and the side-walls of doors, was analyzed.

A total of 8 timelapse sequences of growth cones interacting with doors of various lengths and widths were analyzed (sample sizes shown in Table 1). Three regions were defined within

corridors with doors, as diagrammed in Figure 4A. Figure 4B shows a representative example of an axon and its growth cone before, during and after passing through a door. Growth cones encountering spatial constraints exhibited two types of responses. Growth cones either stopped advancing and extended filopodia and lamellipodia to either side of the growth cone, or underwent lateral displacements along the obstacle until a way around the spatial constraint was encountered. Growth cones that stopped advancing navigated around the spatial constraint when a filopodium or lamellipodium was able to continue extending without further contact with spatial constraints. Consistent with the lack of an effect of door width on axon length (see above), no obvious correlations were evident between door width (8–15μm) and the behavior of growth cones contacting spatial constraints.

Measurements of growth cone area revealed a transient decrease in growth cone size while the axon was navigating though a door as depicted in Figure 4C (see Figure 4B for an example from a timelapse sequence). Growth cone area diminished as the growth cone approached a door, and increased as a growth cone passed through a door into the post-door area. Filopodial and lamellipodial contacts with the walls of the chamber were recorded in each video analyzed. A relationship was noted between growth cone area at a given frame of a timelapse series and the number of contacts made on the previous frame in that series. Neurons simultaneously making at least two contacts with spatial constraints exhibited a decrease in surface area in the next frame observed, while neurons making one or no contacts exhibited an increase in growth cone area in subsequent frames (Figure 4D). T-tests indicated significant differences in area between growth cones making 2 contacts relative to growth cones making 0 or 1 contacts ($p<0.05$ in both instances), indicating that changes in growth cone area depend on the number of contacts made by the growth cone during interactions with spatial constraints.

The decrease in growth cone area observed during interactions with spatial constraints could be due to the decrease in the rate of axon advance during navigation around spatial constraints. If this were the case, then growth cone surface area should correlate with the rate of axon advance when growth cones are extending in the absence of spatial constraints. Five videos of axons extending in the periphery of rectangular chambers were analyzed to compare changes in growth cone and axon dynamics in the periphery to those seen in chambers. Growth cones showed significant changes in area as they grew across a uniform substratum, but no relationship between rate of axon advance and the area of a growth cone was detected (Figure 4E) with growth cones from slowly advancing axons exhibiting approximately the same surface area as growth cones of more rapidly advancing axons. These data are consistent with a previous report on the lack of a correlation between axon advance rates and changes in growth cone surface area [13].

These data suggest that growth cone navigation around spatial constraints involves growth cone sampling through filopodial and lamellipodial protrusion. Decreases in area occurred consistently only when multiple filopodia made contact with spatial obstacles. These data indicate that growth cones sample spatial constraints and when spatial constraints are detected the growth cone undergoes a decrease in area. A decrease in area is the hallmark of molecular guidance cues that repel growth cones [14], a phenomenon termed growth cone collapse. Thus, growth cones respond to contact with spatial constraints through partial collapse.

3.5 Axon navigation around corners

In preliminary work using additional 3-D designs we observed that axons were capable of turning around corners in corridors (Figure 5A). In order to systematically address the issue of the ability of axons to extend around corners, we developed corridors with corners exhibiting angles ranging from 45–135 degrees. Corridors with corners were generated using corridor widths ranging from 20–50 μm. An analysis of the frequency of axon turning, revealed that axons were able to navigate around corners within the full range of angles tested. Axons turned

with frequencies ranging between 50–60%, 60–85% and 75–95% when encountering corners in corridors of 45, 90 and 135 degrees, respectively, depending on corridor width. In general, the frequency of successful axon navigation around corners was greatest at the more obtuse angles (i.e., 135 degrees relative to 45 degrees).

Axons were relatively uniform in their ability to turn around 45 degree corners independent of chamber width (Figure 5B). When turning around 90 degree corners axons exhibited a negative trend toward decreased turning frequencies with increasing corridor width (Figure 5B), but no statistically significant differences were observed. At 90 degree corners, the only statistically significant difference between corridors of different widths was observed comparing 20 to 50 μm widths (Figure 5B; $p<0.05$, X^2 test). At 135 degree corners, we observed an increasing trend in turning frequency with increasing corridor width, but there were not statistically significant differences between 20 and 50 μm widths (Figure 5B). Axons that did not turn around corners were observed to appear stalled at the corner with their growth cones abutting one of the walls of the corridor. Overall, these data demonstrate that axons can turn around corners in corridors as sharp as 45 degrees, but indicate that shallower angles are easier to navigate around, and that the percentage of axons navigating around a corner can be controlled by varying the angle and the width of the corridor.

4. Discussion

Investigations of the mechanism of axon guidance have revealed numerous extracellular signals that control axon behavior. These signals work through specific ligand-receptor interactions and are of great relevance to guidance *in vivo*. However, the presence of a mechanism in growth cones for degrading the extracellular matrix also suggests that growth cones must remove physical constraints present in the organization of the extracellular matrix in order to extend, as suggested by studies of the inhibitory effects of increased matrix porosity on axon extension [2,3]. We developed a model system for studying the interactions of axons and growth cones with 3-D spatial constraints. Our model system shares many similarities with designs of microfluidic chambers, and the information learned from our study should be directly applicable to the design of chambers that combine microfluidics with 3-D constraint-mediated regulation of axon guidance and extension.

Culturing neurons in fully confined chambers 40×40 to 70×70 μm in size decreased the percentage of neurons that established axons. Our expectation was that axons would form and fill the available space within the chambers, or perhaps simply be stunted in total length. The decreased percentage of neurons exhibiting axons in confined chambers was due to the presence of 3-D constraints in all four possible directions of axon extension. Indeed, if neurons were provided with a possible direction to extend an axon they were able to extend axons equivalent to control neurons on a 2-D substratum devoid of spatial constraints. The effects of spatial constraints on axon formation was not likely due to cell death or adverse effects on neurons in general. The ability of some axons to escape the spatial confinements and extend on the top surface of the chips indicates that neurons in confinement were capable of extending long axons. In addition, pharmacological inhibition of myosin II, an enzyme that generates cellular contractile forces, removed the effects of spatial constraints and neurons in small chambers formed axons with frequencies not different from those of neurons on 2D substrata. We suggest that the decrease in axon formation in enclosed chambers is reflective of nascent growth cones interacting with walls and resulting in retraction of the axon back into the cell body. Axons in larger chambers would then persist if the neuron has to generate a minimal amount of axon length prior to encountering a wall in order for the axon to be maintained following contact with a spatial constraint. Overall our observations are consistent with those of Mahoney et al [15] who studied PC12 cell neurite formation and observed that contact with walls in 3-D microfluidic-type chambers inhibited axon extension.

In order to gain insights into the responses of growth cones to spatial constraints, we directly imaged living growth cones interacting with the walls of chambers and doors. Growth cones sampled spatial constraints using filopodial protrusions. Contact of multiple filopodia with walls correlated with a decrease in growth cone area. Decreases in growth cone area are the hallmark of the effects of signals that inhibit axon extension [14]. These observations indicate that growth cones sense 3-D physical constraints in a contact dependent manner. Contact with constraints is then translated into decreased growth cone size and decreased axon extension. Decreases in growth cone area and protrusive activity have long been known to mediate growth cone turning away from repellent molecular guidance cues, and only partial decreases in area are required for guidance [16]. Our observations indicate that the interaction of filopodia with spatial constraints may activate mechanisms within growth cones similar to those used by repellent guidance cues. The response to contact with physical constraints likely involves mechanoreception by growth cones. Indeed, calcium influx through mechanosensitive channels in growth cones has recently been demonstrated to inhibit axon advance [17]. In future work it will be of interest to determine the cellular mechanisms and signaling pathways required for growth cones to respond to spatial constraints.

We tested whether myosin II activity is required for the inhibition of axon establishment imposed by culturing neurons in small chambers (40×40 to 70×70 μm). Inhibition of myosin II allowed neurons to establish axons in small chambers. Myosin II is involved in axon retraction [18]. Thus, myosin II may allow neurons to extend axons in small chambers by decreasing the retraction of axons back into the cell body after contact with a physical constraint. This possibility is not directly supported by the observation that we did not detect axon retraction following contact with walls in live imaging studies. However, retraction may only occur when a growth cone samples a spatial constraint for a prolonged time period, as would be the case with neurons confined in chambers. In our imaging studies, growth cones interacted with spatial constraints only briefly until they detected a region free of spatial constraints and then moved past the constraint. Alternatively, inhibition of myosin II may also promote the branching of axons (unpublished data, H. Francisco and G. Gallo). Increased axon branching following myosin II inhibition may allow neurons to extend more branches and thus have a greater probability of establishing an axon. In addition, inhibition of myosin II may compromise aspects of the intracellular mechanism that transduces contact with a physical constraint into a cellular response.

Axons were able to navigate around corners in corridors. These observations indicate that the guidance of axons from one region of a patterned substratum to another can be controlled by the geometry of the pattern. For example, if only 50% of axons are desired to make a turn in a different direction after having extending to a specific point, our data indicate that 45 degree angles would achieve this degree of guidance. Thus, by controlling the angle of corners in corridors it should be possible to design patterns that result in specific guidance of axons from one point to another.

The length of axons can be controlled by physical constraints. Axons extending through corridors, punctuated by physical constraints in the form of doors, exhibited shorter lengths than axons growing in corridors of the same widths but without additional physical constraints. Live imaging studies of growth cones interacting with physical constraints while navigating between chambers separated by doors revealed that growth cones spend prolonged time periods interacting with the physical constraints around a door until they find a way around the spatial constraint. The increase in the time axons spent navigating through doors, relative to axon extension in corridors without doors, likely explains the shorter lengths of axons extending between chambers through doors.

Longer doors facilitated axon extension relative to shorter doors. This relationship may be attributable to a 'funneling' effect. Once the growth cone has detected the door and starts to move through it, it will encounter only one direction to extend within. Thus, growth cones may advance faster through longer doors due to the absence of alternative paths, which would delay axon extension as the growth cone stalls and seeks alternative routes. These observations indicate that the length of doors is a parameter relevant to regulating the length of axons using physical constraints.

The use of 3-D constraints to guide axons is likely to be of great use in the design of microfluidic systems that rely on similar 3-D substratum manufacturing technologies. Microfulidic systems yield great promise for the next generation of attempts at the generation of *in silico* computational chips using living neurons as the computational units. The establishment and extension of axons in these systems could be controlled by physical aspects of the chamber itself, as well as in combination with substrata patterned by biologically active molecules [8]. Our study demonstrates that the physical constraints inherent in photolithographically constructed microfluidic systems are sufficient for controlling various aspects of axon formation and extension. Thus, it should be feasible to design patterns of 3-D constraints that guide and regulate axon extension in order to build specific geometries of neuronal morphology and connectivity patterns between different neurons *in vitro*. Furthermore, knowledge gained by studying the interactions of sensory growth cones with 3-D constraints may assist in the design of conduits for regenerating sensory axons, which are faced with the task of undergoing guidance and growth into 3-D tubes of Schwann cells in injured nerves [9].

5. Conclusion

In conclusion, in this report we demonstrate that 3-D constraints can be used to guide axons and that 3-D constraints provide a flexible approach to axon guidance. While these results do not demonstrate a significance for spatial constraints *in vivo*, they raise the possibility that during growth cone guidance 3-D aspects of the extracellular environment may contribute to guidance. For example, growth cones may encounter barriers of extracellular matrix that they are not capable to proteolytically digest and thus be unable to navigate through. The *in vitro* model system we characterized will be useful in future studies to dissect the cellular basis of axon guidance by 3-D spatial constraints. The ability to perform live-imaging studies of growth cone encounters with 3-D constraints will greatly assist in these endeavors.

Acknowledgements

This work was supported by NIH grant NS048090 to GG and a Drexel University Synergy grant to GF and GG. The authors thank members of the Friedman laboratory for assistance with the photolithography.

List of References

1. Chisholm A, Tessier-Lavigne M. Conservation and divergence of axon guidance mechanisms. Curr Opin Neurobiol 1999;9:603–15. [PubMed: 10508749]
2. Bellamkonda R, Ranieri JP, Bouche N, Aebischer P. Hydrogel-based three-dimensional matrix for neural cells. J Biomed Mater Res 1995;29:663–71. [PubMed: 7622552]
3. Dillon GP, Yu X, Sridharan A, Ranieri JP, Bellamkonda RV. The influence of physical structure and charge on neurite extension in a 3D hydrogel scaffold. J Biomater Sci Polym Ed 1998;9:1049–69. [PubMed: 9806445]
4. McFarlane S. Metalloproteases: carving out a role in axon guidance. Neuron 2003;37:559–62. [PubMed: 12597854]
5. Nordstrom LA, Lochner J, Yeung W, Ciment G. The metalloproteinase stromelysin-1 (transin) mediates PC12 cell growth cone invasiveness through basal laminae. Mol Cell Neurosci 1995;6:56–68. [PubMed: 7599958]

6. Rajnicek A, McCaig C. Guidance of CNS growth cones by substratum grooves and ridges: effects of inhibitors of the cytoskeleton, calcium channels and signal transduction pathways. J Cell Sci 1997;110:2915–24. [PubMed: 9359874]
7. Rajnicek A, Britland S, McCaig C. Contact guidance of CNS neurites on grooved quartz: influence of groove dimensions, neuronal age and cell type. J Cell Sci 1997;110:2905–13. [PubMed: 9359873]
8. Li N, Folch A. Integration of topographical and biochemical cues by axons during growth on microfabricated 3-D substrates. Exp Cell Res 2005;311:307–16. [PubMed: 16263111]
9. Witzel C, Rohde C, Brushart TM. Pathway sampling by regenerating sensory axons. J Comp Neurol 485:183–190. [PubMed: 15791642]
10. Gallo G, Lefcort FB, Letourneau PC. The trkA receptor mediates growth cone turning toward a localized source of nerve growth factor. J Neurosci 1997;17:5445–54. [PubMed: 9204927]
11. Brown ME, Bridgman PC. Myosin function in nervous and sensory systems. J Neurobiol 2004;58:118–30. [PubMed: 14598375]
12. Straight AF, Cheung A, Limouze J, Chen I, Westwood NJ, Sellers JR, Mitchison TJ. Dissecting temporal and spatial control of cytokinesis with a myosin II Inhibitor. Science 2003;299:1743–7. [PubMed: 12637748]
13. Gallo G, Pollack ED. Cyclic remodelling of growth cone lamellae and the effect of target tissue. Brain Res Dev Brain Res 1995;85:140–5.
14. Gallo G, Letourneau PC. Regulation of growth cone actin filaments by guidance cues. J Neurobiol 2004;58:92–102. [PubMed: 14598373]
15. Mahoney MJ, Chen RR, Tan J, Saltzman WM. The influence of microchannels on neurite growth and architecture. Biomaterials 2005;26:771–8. [PubMed: 15350782]
16. Fan J, Raper JA. Localized collapsing cues can steer growth cones without inducing their full collapse. Neuron 1995;14:263–74. [PubMed: 7857638]
17. Jacques-Fricke BT, Seow Y, Gottlieb PA, Sachs F, Gomez TM. Ca2+ influx through mechanosensitive channels inhibits neurite outgrowth in opposition to other influx pathways and release from intracellular stores. J Neurosci 2006;26:5656–64. [PubMed: 16723522]
18. Chantler PD, Wylie SR. Elucidation of the separate roles of myosins IIA and IIB during neurite outgrowth, adhesion and retraction. IEE Proc Nanobiotechnol 2003;150:111–25. [PubMed: 16468940]

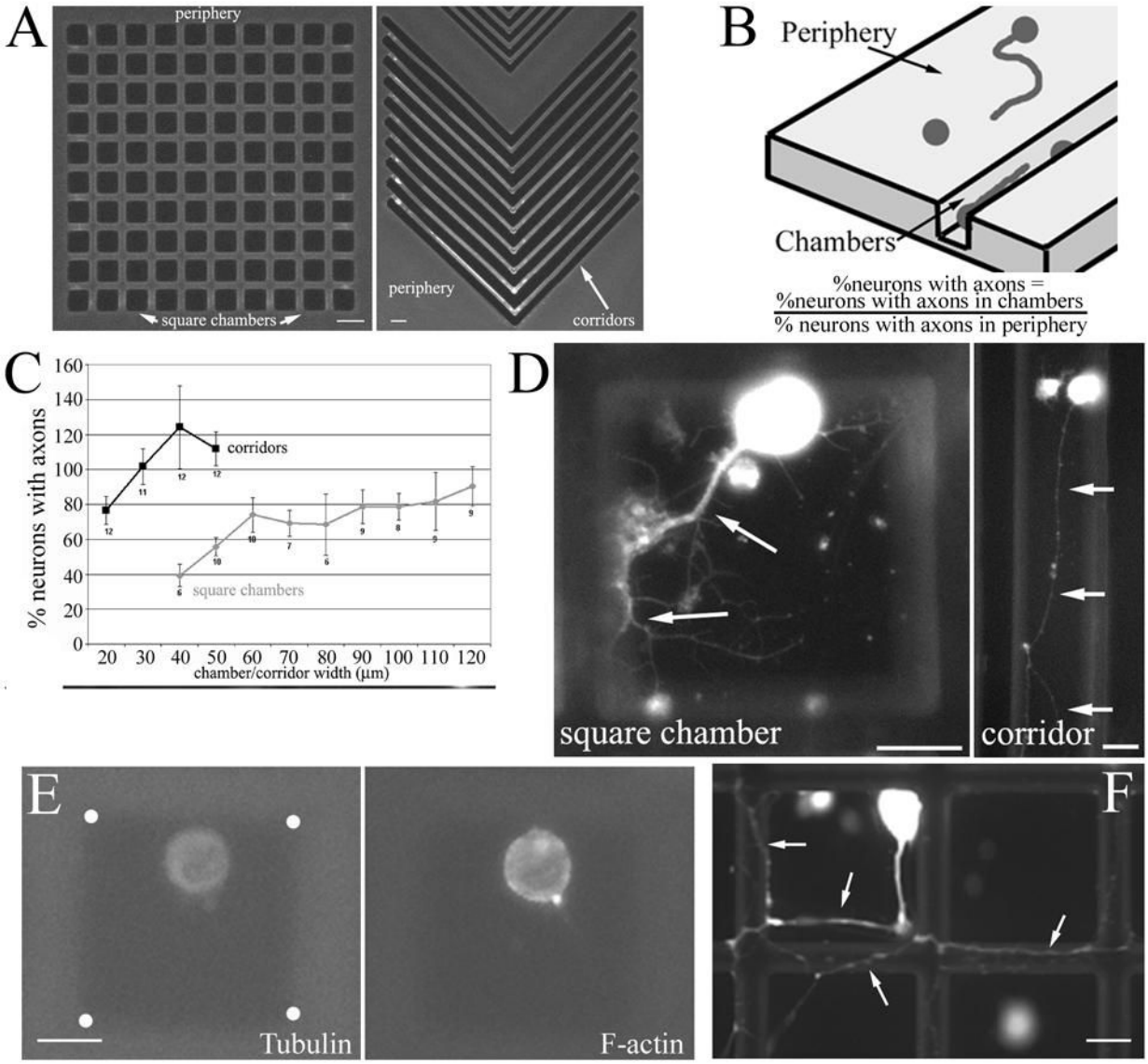

Figure 1.

Regulation of axon formation by 3-D constraints. (A) Example of photolithographically generated patterns of 3-D constraints in the form of square chambers and corridors (here shown with corners). Bars = 40 and 20 μm, respectively. (B) Diagram of metric for determining the relative percentage of neurons with axons in chambers and on the periphery. The relative % of neurons extending axons under conditions of confinement is determined by dividing the percentage of neurons in chambers that have axons by the percentage of neurons in the periphery of the same chip that have axons. (C) The percentage of neurons with axons presented as a function of square chamber and corridor width. Cells were immunocytochemically stained with anti-tubulin antibodies. Confinement in square chambers inhibits axon growth from neuronal cell bodies. Confinement in corridors did not significantly decrease axon growth and the values obtained for 20–50 μm did not differ from one another (ANOVA, $p>0.2$). n=arrays of chambers. (D) Examples of neurons with axons (arrows) in square chambers and corridors. Bars = 20 μm. (E) Example of a neuron in a square chamber without an axon. The positioning of the cell body within the chamber is similar to that in the example shown in panel D. However,

no axon is visible as determined by staining against tubulin or actin filaments (phalloidin stain). These images are dimmer than those in panel D because a shorter exposure was used to obtain pictures for panel E since the cells had no axon, and the cell body is thus not saturated in the tubulin channel as it is in panel D. White dots in the tubulin panel denote the corners of the chamber. Bar = 20 μm. (F) Example of an ‘escapee’ neuron that was able to extend its axon (arrows) onto the surface of the chip. Focus is on the surface of the chip. Bar = 20 μm.

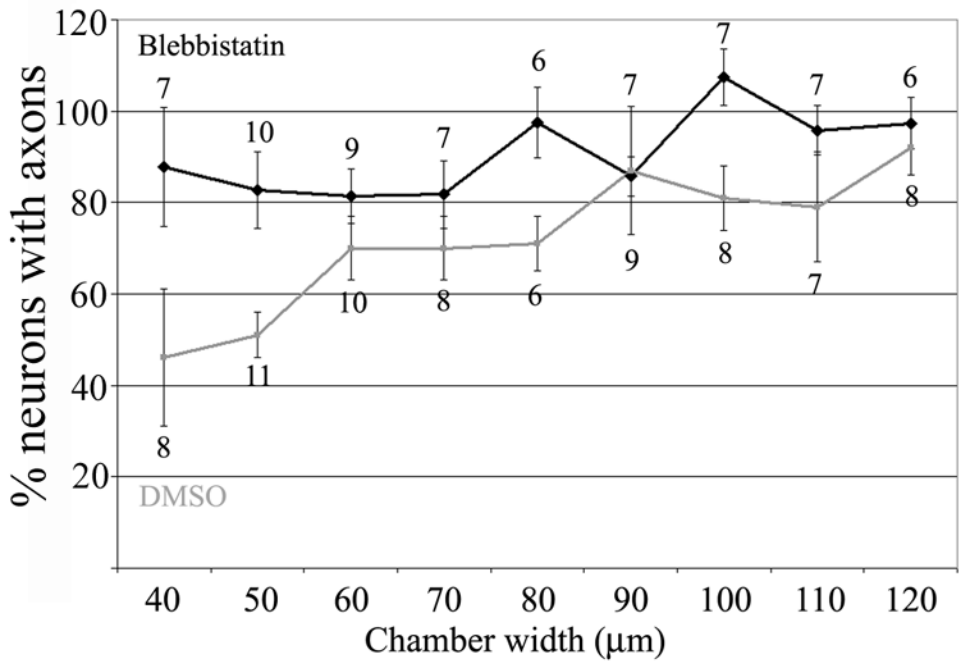

Figure 2.

Inhibition of myosin II allows formation of axons in 3-D confinement. Culturing neurons in the presence of the myosin II inhibitor blebbistatin allows neurons to form axons in square chambers of small width. Analysis was performed as in Figure 1. Treatment with DMSO did not alter the response to confinement relative to no treatment, compare to data from chambers in Figure 1B. n= arrays of chambers.

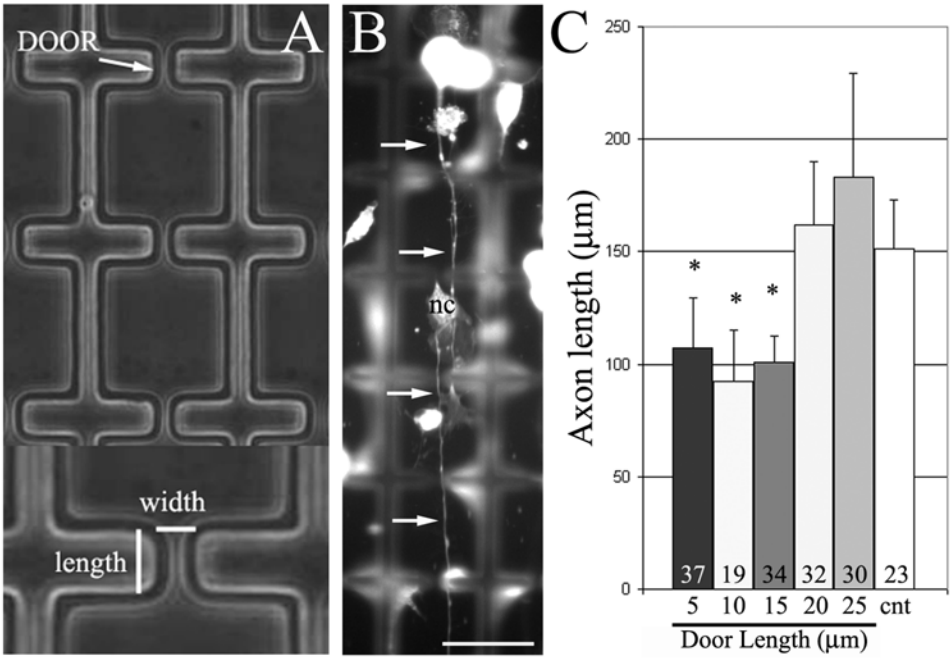

Figure 3.

Axon length can be controlled using 3-D constraints. (A) Example of corridors with doors. Doors are described by their width and length. (B) Example of neuron extending axon (arrows) through multiple doors in a corridor. Some non-neuronal cells, fibroblasts, from the DRG are also present (labeled, nc). Focus is on the 'floor' of the corridor and walls are out of focus. Bar = 40 μm. (C) Graph of axon length as a function of door length. Doors of lengths less than 20 μm resulted in shorter axons than controls extending in corridors without doors (cnt). Numbers of axons analyzed per group is shown in the bars. Cells were immunocytochemically stained with anti-tubulin antibodies.

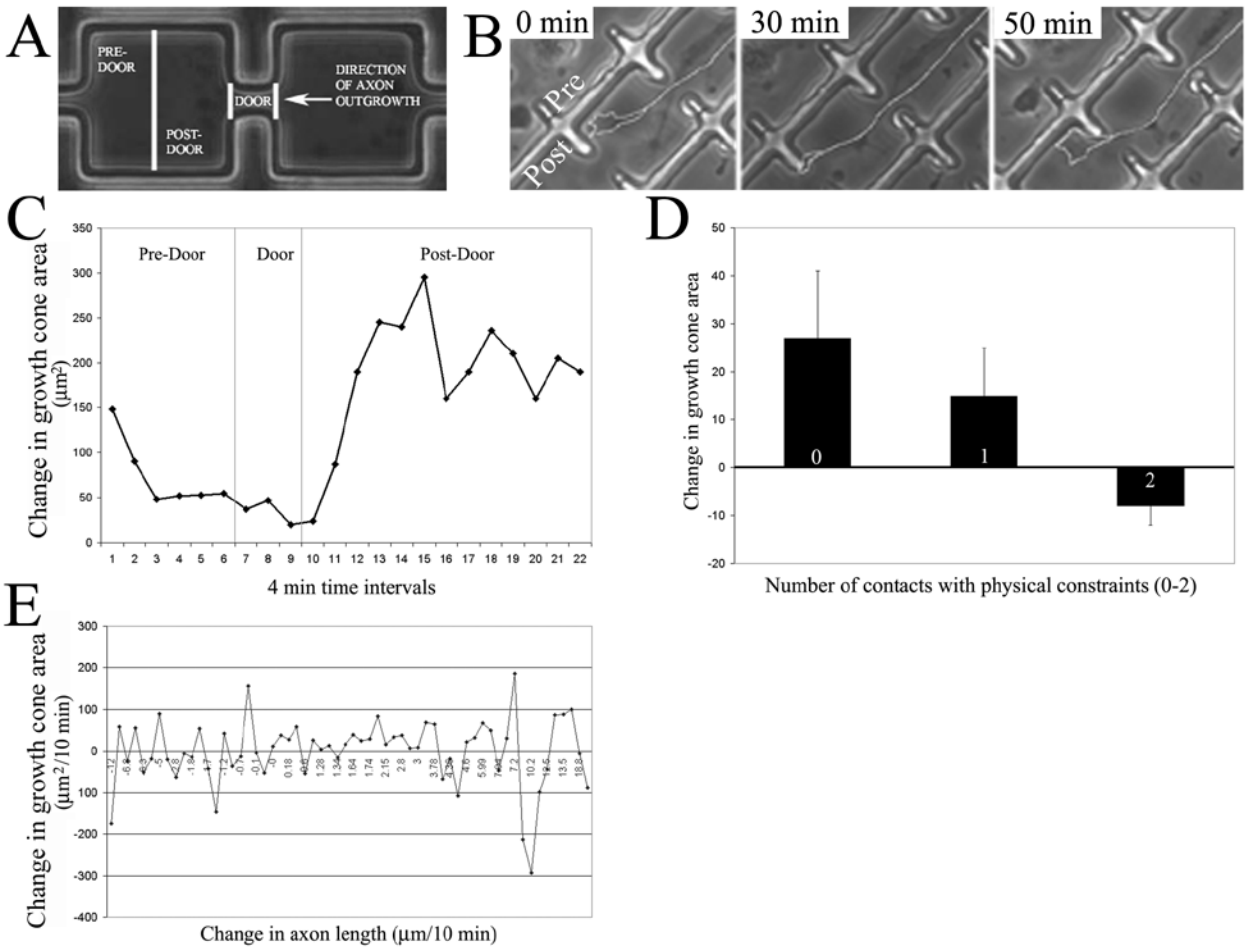

Figure 4.

Live imaging of growth cone interactions with 3-D constraints. (A) Schematic of the nomenclature used to refer to corridors with doors. (B) Sequence from a timelapse video of a growth cone navigating through a door. At 0 min the growth cone is facing a corner next to the door in the pre-door region (Pre and Post regions labeled in this panel). By 30 min the growth cone has displaced laterally toward the door. By 50 minutes the growth cone has navigated through the door and is in the post-door region of the next section of the corridor. The axon and growth cone were traced in white for presentation purposes. (C) Representative graph of growth cone area as a function of time and position during navigation through a door. In the pre-door region the growth cone became progressively smaller while interacting with physical constraints. While extending through the door the growth cone area was minimal. However, the area of the growth cone increased when the growth cone passed through the door and entered the post-door region. (D) The number of contacts made by growth cones with physical constraints correlated with decreases in growth cone area after the contact. The percent change in area observed 1 minute after contact was observed is shown. (E) Graph showing the lack of a relationship between growth cone area and the rate of axon advance on a 2D substratum. Each datum represents one growth cone imaged for a ten-minute period during which both variables were measured.

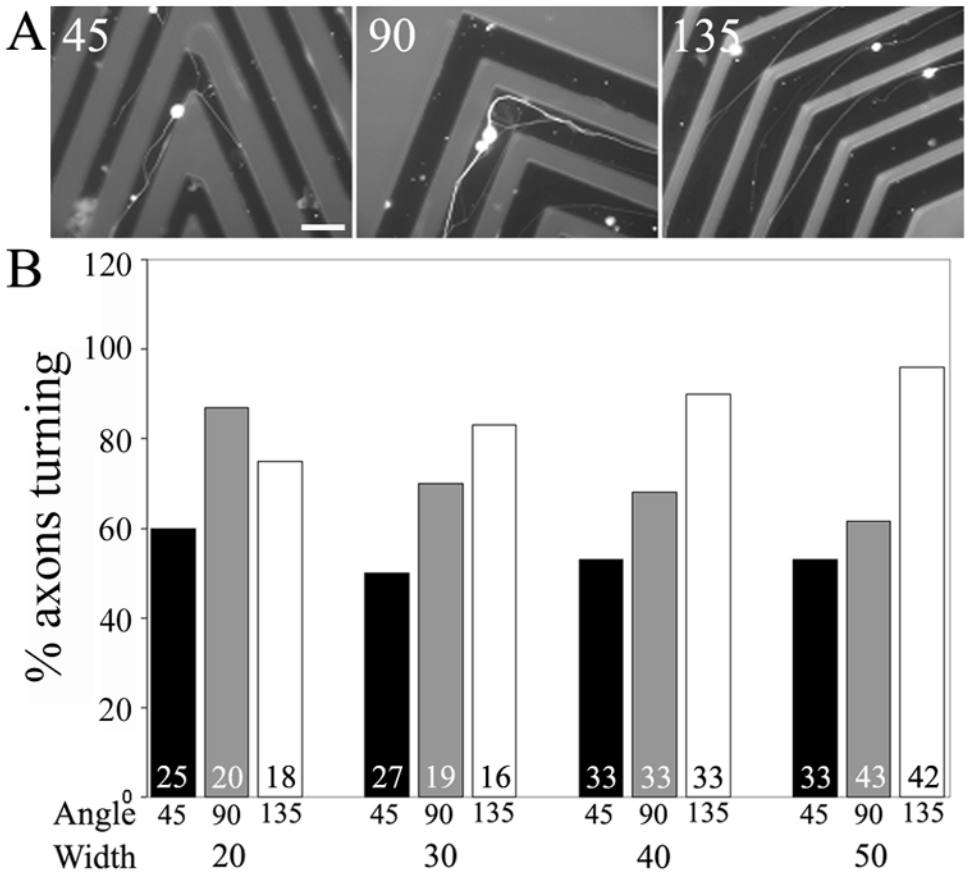

Figure 5.

Axons navigate around corners in corridors. (A) Examples of axons that navigated around corners (45, 90 and 135 degrees). Bar = 50 μm. (B) Graph of the percentage of axons that navigated around corners as a function of corner angle and corridor width (μm). Numbers in bars reflect axons scored. Cells were immunocytochemically stained with anti-tubulin antibodies.

Table 1

Number of axons analyzed	Door width (W) and length (L)
2	W15 L20
2	W15 L10
1	W15 L5
1	W10 L25
1	W10 L15
1	W10 L5